Insight into the Family of Na^+/Ca^{2+} Exchangers of *Caenorhabditis elegans*

Vishal Sharma,*,† Chao He,*,† Julian Sacca-Schaeffer,* Eric Brzozowski,* Daniel E. Martin-Herranz,‡ Zelda Mendelowitz,*,† David A. Fitzpatrick,‡ and Damien M. O'Halloran*,†,1

*Department of Biological Sciences, The George Washington University, Washington, DC 20052, †Institute for Neuroscience, The George Washington University, Washington, DC 20052, and ‡Department of Biology, Genome Evolution Laboratory, National University of Ireland Maynooth, Maynooth, County Kildare, Ireland

ABSTRACT Here we provide the first genome-wide *in vivo* analysis of the Na^+/Ca^{2+} exchanger family in the model system *Caenorhabditis elegans*. We source all members of this family within the *Caenorhabditis* genus and reconstruct their phylogeny across humans and *Drosophila melanogaster*. Next, we provide a description of the expression pattern for each exchanger gene in *C. elegans*, revealing a wide expression in a number of tissues and cell types including sensory neurons, interneurons, motor neurons, muscle cells, and intestinal tissue. Finally, we conduct a series of behavioral and functional analyses through mutant characterization in *C. elegans*. From these data we demonstrate that, similar to mammalian systems, the expression of Na^+/Ca^{2+} exchangers in *C. elegans* is skewed toward excitable cells, and we propose that *C. elegans* may be an ideal model system for the study of Na^+/Ca^{2+} exchangers.

CALCIUM functions as a diverse signaling molecule in a variety of cell types through activation and conformational changes of proteins, as well as via modulation of cellular capacitance (Berridge *et al.* 2000, 2003; Bootman *et al.* 2001). Neurotransmitter release, muscular contraction, apoptosis, and lymphocyte activation are some of the many cellular processes mediated by calcium signaling, and accordingly, strict balance of calcium levels must be maintained to prevent cellular dysfunction. Cells accomplish this primarily by extruding calcium through plasma membrane-embedded plasma membrane Ca^{2+} ATPase (PMCA) pumps and utilizing exchanger ion transporters. PMCA proteins are high-affinity/low-capacity pumps that maintain calcium homeostasis over sustained periods of time by removing one Ca^{2+} ion for every ATP hydrolyzed (Tidow *et al.* 2012). Exchangers such as Na^+/Ca^{2+} exchangers (NCX), $Na^+/Ca^{2+}/K^+$ exchangers (NCKX), and calcium/cation exchangers (CCX) are low-affinity/high-capacity ion transporters that rapidly expel calcium ions (Philipson and Nicoll 2000; Philipson *et al.* 2002; Lytton 2007; Nicoll *et al.* 2013). The NCX, NCKX, and CCX families of exchangers comprise the three branches of the family of Na^+/Ca^{2+} exchangers in animals (Cai and Lytton 2004a,b; Lytton 2007). Under normal physiological conditions, NCX ion transporters utilize the energy stored in the transmembrane gradient to allow influx of three Na^+ ions and extrusion of one Ca^{2+} ion (Hilge 2012; Ottolia and Philipson 2013). In the case of the NCKX transporter, there is one Ca^{2+} and one K^+ ion exchanged in return for Na^+ ion influx, and in the case of the CCX exchangers, both Na^+/Ca^{2+} and Li^+/Ca^{2+} exchanges have been observed (Lytton. 2007; Visser and Lytton 2007). As of yet, the nematode *Caenorhabditis elegans* has not been used as an *in vivo* model organism to study the NCX, NCKX, CCX exchanger family. Here we provide a detailed description of the phylogeny of this family of transporters in *C. elegans*, examine the expression patterns of each member, and uncover roles for one NCX member and one CCX member in muscle contractions, lipid accumulation, and longevity in *C. elegans*. Our results show that exchanger proteins are widely expressed in a number of tissues and cell types in *C. elegans* including sensory neurons, interneurons, motor neurons, muscle cells, and intestinal tissue, and we propose that *C. elegans* may be an ideal *in vivo* model system to contribute to our understanding of Na^+/Ca^{2+} exchanger biology.

doi: 10.1534/genetics.113.153106
Manuscript received May 13, 2013; accepted for publication July 17, 2013
Supporting information is available online at http://www.genetics.org/lookup/suppl/doi:10.1534/genetics.113.153106/-/DC1.
[1]Corresponding author: George Washington University, Ross Hall 636, 2300 I St. NW, Washington, DC 20052. E-mail: damienoh@gwu.edu

Results

Phylogenetic analysis of NCX, NCKX, and CCX transporters in C. elegans

We first performed a detailed phylogenetic characterization of the NCX, NCKX, and CCX genes in *C. elegans*. To identify orthologs and paralogs of these exchangers, we interrogated genomes within the *Caenorhabditis* genus (*C. briggsae*, *C. brenneri*, *C. japonica*, *C. remanei*) and within *Pristionchus pacificus*, *Drosophila melanogaster*, and humans. A total of 10 Na^+/Ca^{2+} exchanger genes were detected in the *C. elegans* genome and are designated *ncx-1*–*ncx-10* at Wormbase (http://www.wormbase.org). Phylogenetic analysis revealed that *ncx-1*, *ncx-2*, and *ncx-3* belong to the NCX family of exchangers (Figure 1A). Orthologs of these three NCX genes were detected throughout the *Caenorhabditis* genus (*i.e.*, in *C. briggsae*, *C. brenneri*, *C. japonica*, and *C. remanei*) with one exception: a clear ortholog of *ncx-3* was missing from *C. brenneri*, suggesting an example of gene loss. Orthologs of all three NCX genes were also detected in the Diplogastridae family member *Pristionchus pacificus*. For *ncx-1* there are two predicted isoforms and for *ncx-2* there are four predicted isoforms in *C. elegans*. In humans there are also three NCX loci (*ncx1*, *ncx2*, and *ncx3*), with *ncx-1* in *C. elegans* being the most closely related NCX transporter to the human orthologs. NCX-2 and NCX-3 in *C. elegans* are more divergent from the human NCX/*C.elegans* NCX-1 cluster. In *Drosophila* we detected only a single NCX gene, called CalX, which is in keeping with previous reports (Cai and Lytton 2004a). Next, we found that *ncx-4* and *ncx-5* in *C. elegans* encode for proteins that belong to the NCKX branch (Figure 1A). Orthologs of the *C. elegans* NCKX members were detected in all *Caenorhabditis* members examined and also in the more divergent nematode species *P. pacificus*. We detected two NCKX orthologs in *Drosophila*, called *nckx30c* and *nckx-X-SC*. Both NCX-4 and NCX-5 in *C. elegans* are more closely related to *nckx30c* in *Drosophila*. Within humans there is an expansion of the NCKX branch to produce five members—NCKX1, NCKX2, NCKX3, NCKX4, and NCKX5. Human NCKX1 and NCKX2 are most closely related to the *C. elegans* NCKX members, and human NCKX3, NCKX4, and NCKX5 form a separate clade that includes the *Drosophila nckx-X-SC* gene. From our phylogenetic analysis we found that the remaining *C. elegans* calcium cation exchanger genes belong to the CCX branch (Figure 1A); these are *ncx-6*, *ncx-7*, *ncx-8*, *ncx-9*, and *ncx-10*. In humans there is one member of this branch named NCKX6, and we detected four uncharacterized members of this branch in *Drosophila melanogaster*: NP_610408.2, NP_001097232.2, NP_610405.3, and NP_611156.3. With the exception of *ncx-8*, which was detected only in *C. briggsae* (CB08638), orthologs of all the *C. elegans* CCX members were detected in all *Caenorhabditis* members examined: *C. briggsae*, *C. brenneri*, *C. japonica*, and *C. remanei*. In the case of *P. pacificus*, we detected orthologs for *ncx-7*, *ncx-8*, *ncx-9*, and *ncx-10*. Synteny of the NCX, NCKX, and CCX genes are highly conserved between *C. elegans* and *C. briggsae* (Figure 1B). The NCKX exchanger *ncx-4* is located on chromosome I; *ncx-6* and *ncx-7* are located on chromosome III; *ncx-3* is located on chromosome IV; and *ncx-1*, *ncx-2*, *ncx-5*, *ncx-8*, *ncx-9*, and *ncx-10* are located on chromosome V for both species. The genomic positions of *ncx-6* and *ncx-7* and also of *ncx-8* and *ncx-9* are consecutive within both genomes, indicating the possibility of more recent gene-duplication events (Figure 1B).

Predicted protein structure of NCX, NCKX, and CCX transporters in C. elegans

We examined the predicted protein structure of all 10 *C. elegans* Na^+/Ca^{2+} exchanger genes and their isoforms using SMART, InterPro, and TM Finder programs (Figure 1C). The *C. elegans* NCX-1, NCX-2, and NCX-3 proteins that form the NCX branch from our phylogenetic analysis all have similar structure to the mammalian NCX exchangers. The *C. elegans* NCX exchanger proteins contain two Na^+/Ca^{2+} exchanger domains that are spanned by multiple transmembrane segments. Between the Na^+/Ca^{2+} exchanger sites is a large intracellular loop (between TM4 and TM5 in NCX-1 and NCX-2 isoforms As), which contains two calcium-binding domains (Figure 1C). NCX-1 isoform A, NCX-1 isoform B, and NCX-2 isoforms A, B, and D contain a signal peptide that is absent in NCX-2 isoform C and NCX-3 (Figure 1C). From our phylogenetic analysis we identified two NCKX exchangers in *C. elegans*: NCX-4 and NCX-5. Both NCKX exchangers have similar protein structures characterized by a large K^+-dependent Na^+/Ca^{2+} exchanger-like domain with multiple transmembrane segments separated by a hydrophilic middle region (Figure 1C). NCX-4 isoform B is the smallest exchanger found within the *C. elegans* Na^+/Ca^{2+} exchanger gene family comprising 154 amino acids and interestingly does not contain a predicted K^+-dependent Na^+/Ca^{2+} exchanger domain but instead is predicted to contain only a single Ca^{2+} exchanger domain. This suggests a surprising level of functional complexity mediated at the transcriptional level within the NCKX branch. The *C. elegans* NCX-6, NCX-7, NCX-8, NCX-9, and NCX-10 exchangers are all structurally distinct from the NCX and NCKX proteins. Although NCX-6, NCX-7, NCX-8, NCX-9, and NCX-10 contain two Na^+/Ca^{2+} exchanger domains similar to the NCX exchanger proteins, they lack calcium-binding domains and have multiple transmembrane segments positioned between both Na^+/Ca^{2+} exchanger domains. NCX-6/NCX-7 and NCX-8/NCX-9 share very similar overall protein structures. A predicted signal peptide is found in NCX-6, NCX-7, NCX-8, and NCX-10 and is absent in NCX-9.

NCX, NCKX, and CCX expression patterns in C. elegans

To examine the tissue and cell distribution of NCX, NCKX, and CCX genes in *C. elegans*, we generated reporter GFP fusions by fusing promoter sequences (Supporting Information File S1, Figure S1 and Table S1) to a GFP gene. Stable transgenic lines expressing these reporters were examined microscopically to identify the cells in which each gene

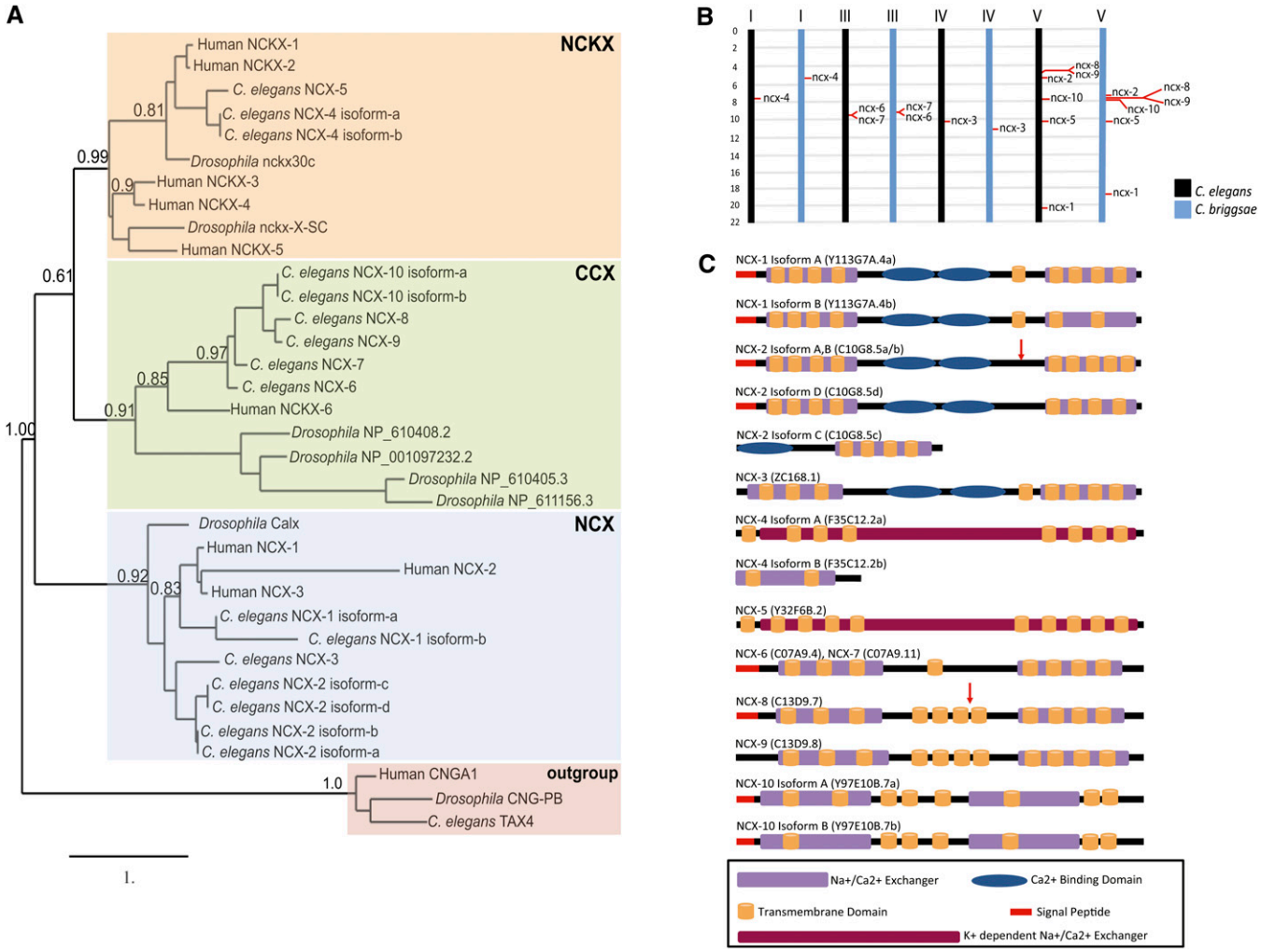

Figure 1 (A) Phylogenetic analysis of NCX, NCKX, and CCX exchangers. Na^+/Ca^{2+} exchangers from *C. elegans*, *D. melanogaster*, and *Homo sapiens* were used to build a phylogeny for this superfamily. The cyclic nucleotide gated channel subunits were used as an outgroup. Genomes were downloaded from Wormbase (*C. elegans*), National Center for Biotechnology Information (*Drosophila*), and Ensembl (human) and interrogated for NCX, NCKX, and CCX exchanger sequences. Orthologs were aligned using the multiple sequence alignment software MUSCLE v3.8.31, and gaps were systematically stripped after alignment. Phylogenetic relationships were inferred by reconstructing trees by maximum likelihood using the PhyML command-line application. The appropriate model was selected using Prottest v.3 and determined to be the "WAG+I+G+F" model with a fixed gamma distribution parameter of 1.5, proportion of invariable sites set to 0.003, and four substitution rate categories. (B) Analysis of synteny between *C. elegans* and its sister species *C. briggsae* for NCX, NCKX, and CCX exchanger genes. Chromosomal coordinates were mined from WormBase. The *C. briggsae* ortholog of *ncx-8* was inferred from bidirectional BlastP searches, phylogenetic analysis, and synteny position to be CBG08638. The *y*-axis numbers indicate mega-base- pair position. (C) Predicted protein structure of NCX, NCKX, and CCX exchangers. Protein structure was determined using SMART database, Interpro database, and the transmembrane prediction program TM Finder. Calcium-binding domains were detected only for the *C. elegans* NCX exchangers (NCX-1, NCX-2, NCX-3). The CCX exchangers (NCX-6, NCX-7, NCX-8, NCX-9, and NCX-10) lack predicted calcium-binding domains and have additional transmembrane segments positioned between the Na^+/Ca^{2+} exchanger domains. The NCKX proteins, NCX-4 and NCX-5, are predicted to contain K^+-dependent Na^+/Ca^{2+} exchanger-like domains. The alternative isoform NCX-4(b) does not contain a predicted K^+-dependent Na^+/Ca^{2+} exchanger domain. Red arrowheads indicate the position of the genetic lesion in *ncx-2(gk879849)* and *ncx-8(gk234217)*.

was expressed (Table 1 and Figure 2). From this analysis we found that the Na^+/Ca^{2+} exchanger genes in *C. elegans* are expressed in very diverse cell types including primary sensory neurons, interneurons, and motor neurons, as well as various pharyngeal, body-wall, and vulval muscle cells. Specific branches of the Na^+/Ca^{2+} exchanger family also exhibited tissue specificity; for example, the NCKX members *ncx-4* and *ncx-5* are exclusively expressed in neuronal cells. These neuronal cells include sensory neurons, interneurons, and motor neuron cells (Table 1 and Figure 2). Interestingly, in the case of *ncx-5* it is not very widely expressed, suggesting a more specific role in sensory neurons: *ncx-5* is expressed in three pairs of amphid neurons called the BAG, URX, and AQR cells as well as in one pair of phasmid neurons called the PQR cells. These neurons are specialized oxygen-sensing cells that play a critical role in social feeding behavior (Coates and De Bono 2002; Gray *et al.* 2004, 2005). The NCX genes *ncx-1*, *ncx-2*, and *ncx-3* are, as

Table 1 Na^+/Ca^{2+} exchanger gene expression patterns in *C. elegans*

Gene	Sequence[a]	Coordinates[b]	Expression pattern in adult hermaphrodites
ncx-1	Y113G7A.4	V:20105601.0.20120644	AIY interneurons
ncx-2	C10G8.5	V:5303671.0.5311230	Pharyngeal muscle including procorpus, metacorpus, isthmus and terminal bulb, body-wall muscle, enteric muscle, vulval muscle
ncx-3	ZC168.1	IV:10716636.0.10721735	Head neurons, dorsal/ventral nerve cord and commissures, phasmid neurons
ncx-4	F35C12.2	I:9808895.0.9813066	AWC, ASE, two pairs of labial neurons, ventral/dorsal nerve cord and commissures, faint expression in one pair of nondye-filling posterior neurons
ncx-5	Y32F6B.2	V:10486450.0.10490025	URX, AQR, and BAG anterior neurons and PQR phasmid neurons
ncx-6	C07A9.4	III:9710165.0.9713844	ADL neuron, intestine
ncx-7	C07A9.11	III:9715799.0.9720207	ADL neuron (faint expression in one other amphid neuron pair), intestine, one pair of posterior cells
ncx-8	C13D9.7	V:4983735.0.4987183	Pharyngeal muscle including procorpus, metacorpus, isthmus and terminal bulb, intestine
ncx-9	C13D9.8	V:4991490.0.4995049	Very faint expression in neurons
ncx-10	Y97E10B.7	V:7930455.0.7933078	Pharyngeal muscle—predominately the terminal bulb

[a] Identifier at http://www.wormbase.org.
[b] Indicates the chromosome number and genomic region.

a family, not restricted to a specific tissue, but individually they are. The *ncx-1* and *ncx-3* are exclusively expressed in neurons, while *ncx-2* is expressed only in non-neuronal cells including the pharyngeal tissue, enteric muscle, and vulval muscle (Figure 2B). The CCX genes exhibit much more diversity in their expression patterns, which is similar to the CCX transporter in humans (Cai and Lytton 2004a,b). The CCX class gene *ncx-6* is expressed in a pair of head neurons termed the ADL and also in the intestine (Table 1 and Figure 2). The ADL amphid neurons play a role in detecting high concentrations of toxic heavy metals (Cu^{2+} and Cd^{2+}) and repellant odors, avoiding high oxygen levels, and regulate social feeding behavior (Troemel *et al.* 1995; Sambongi *et al.* 1999). The *ncx-7* gene is also expressed in the ADL neuron pair and was also detected more faintly in another pair of amphid neurons as well as the intestine and one pair of posterior neurons. The CCX exchanger *ncx-8* is expressed strongly in the intestinal cells and also in the pharyngeal *muscle*, *ncx-9* was faintly expressed in neurons particularly in the head region, and finally *ncx-10* was detected only in pharyngeal muscle cells (Table 1 and Figure 2).

Behavioral analysis of ncx-2 and ncx-8 mutant animals

To functionally characterize Na^+/Ca^{2+} exchangers in *C. elegans*, we obtained mutants in the *ncx-2* (NCX) and *ncx-8* (CCX) genes. The lesion and gene structure for each mutant is illustrated in Figure 3, A and F. In each case a single base-pair mutation resulting in a premature stop codon defines the lesion, and in each case it occurs before the C-terminal exchanger domain (see red arrowheads in Figure 1C). To understand the function of each gene, we examined behaviors based upon the expression pattern of each gene. In the case of *ncx-2* we observed strong expression in the pharynx, body-wall muscle, vulval muscle, and enteric muscles (Figure 2B). We reasoned that examining the defecation motor program (DMP) cycle in these mutants may uncover a role for NCX-2 in regulating rhythmical motor programs. The DMP cycle is a stereotyped sequence of muscle contractions and occurs approximately every 45 sec (Thomas 1990). In the adult hermaphrodite the defecation program begins with the contraction of the posterior body-wall muscles, which increases internal pressure; this contraction lasts for only ~1 sec, and upon relaxation of these muscles the intestinal contents flow posteriorly, thereby allowing the intestinal contents to collect in the pre-anal region. Finally, the contents of the pre-anal region are expelled by contraction of the enteric muscles. We assayed *ncx-2(gk879849)* and wild-type animals cultivated on bacteria expressing double-stranded RNA (dsRNA) targeting *ncx-2*, and in each case we observed a significant delay in the number of expulsions per DMP cycle when compared with wild-type animals [Figure 3B: $P < 0.005$ for wild-type *vs.* *ncx-2(gk879849)* mutants; $P < 0.005$ for wild-type *vs.* *ncx-2(RNAi)* animals]. We also observed strong expression of *ncx-2* in vulval muscle, and so next we examined the rate of egg laying for *ncx-2 (gk879849)* mutants and wild-type animals cultivated on bacteria expressing dsRNA targeting *ncx-2* (Figure 3C). In each case, we observed significantly reduced egg-laying frequency in the *ncx-2* mutant background [Figure 3C: $P < 0.05$ for wild-type *vs.* *ncx-2(gk879849)* mutants; $P < 0.05$ for wild-type *vs.* *ncx-2(RNAi)* animals]. We also examined the number of fertilized unlaid eggs for *ncx-2(gk879849)* mutants compared with those for wild-type animals and found that *ncx-2* mutants do not lay fewer eggs due to a lack of eggs in the uterus but also do not accumulate more eggs [mean number of unlaid eggs for wild type = 12 ± 0.6 and mean for *ncx-2(gk879849)* = 9 ± 0.4]. We also observed expression of *ncx-2* in body-wall muscle and tested a role for NCX-2 in locomotion behavior. To this end, we examined the speed of movement for *ncx-2(gk879849)* mutant animals

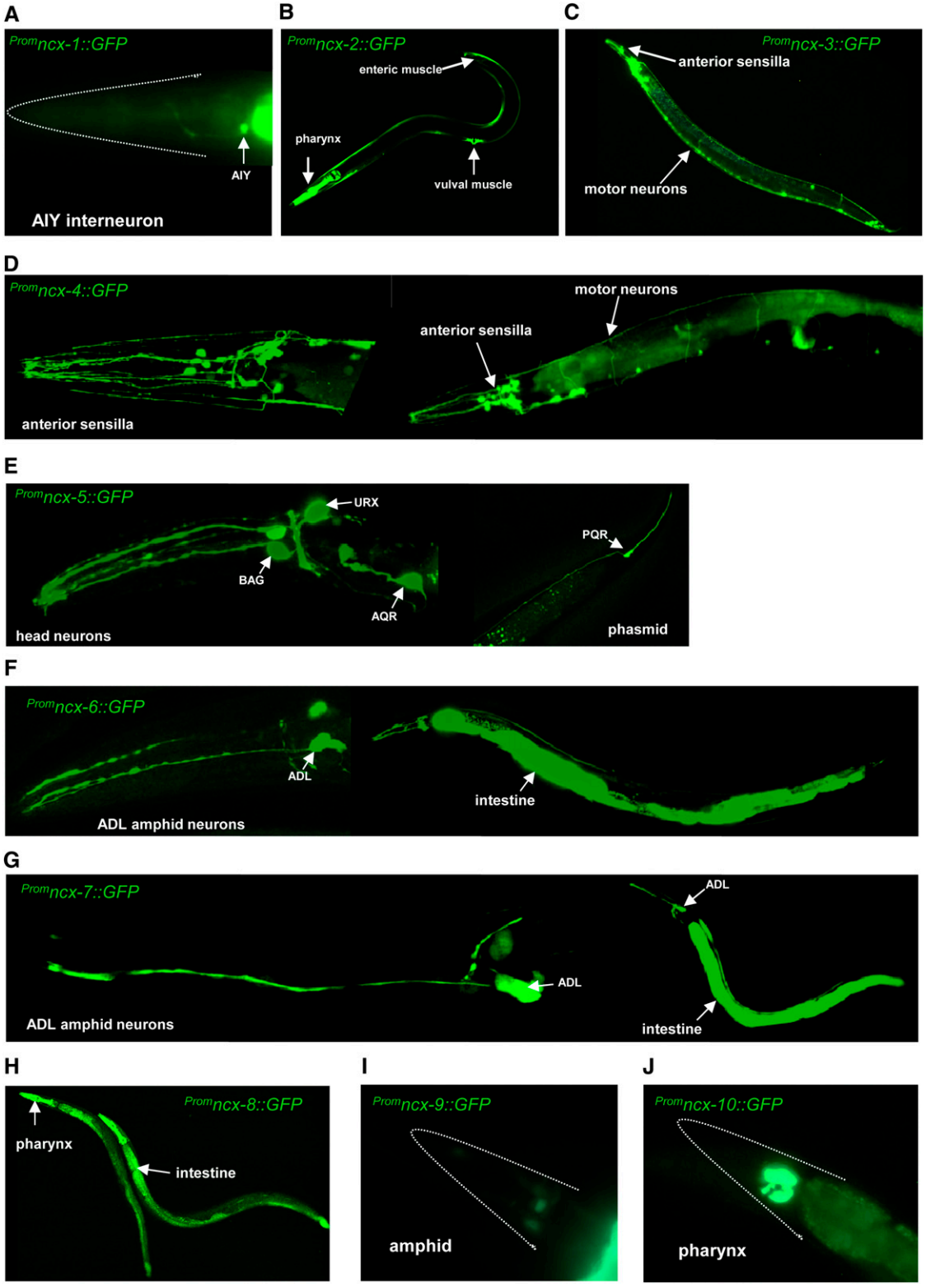

Figure 2 NCX, NCKX, and CCX exchanger genes are widely expressed in *C. elegans*. Stable transgenic lines expressing GFP reporter fusions were imaged, and representative images are shown from reporter lines expressing the following fusions: (A) *(p)ncx-1*::*GFP*; (B) *(p)ncx-2*::*GFP*; (C) *(p)ncx-3*::*GFP*; (D) *(p)ncx-4*::*GFP*; (E) *(p)ncx-5*::*GFP*; (F) *(p)ncx-6*::*GFP*; (G) *(p)ncx-7*::*GFP*; (H) *(p)ncx-8*::*GFP*; (I) *(p)ncx-9*::*GFP*; and (J) *(p)ncx-10*::*GFP* are shown to illustrate the diversity of tissues and cell types that express the NCX (*ncx-1*, *ncx-2*, *ncx-3*), NCKX (*ncx-4 and ncx-5*), and CCX (*ncx-6*, *ncx-7*, *ncx-8*, *ncx-9*, and *ncx-10*) genes in *C. elegans*. All images are from day 1 or day 2 adults. In A, I, and J, the white dotted line indicates the anterior head region of the animal. For all images, left is anterior and dorsal is up. In D, F, and G, whole-body images are to the right, and zoomed-in images of the anterior region are to the left.

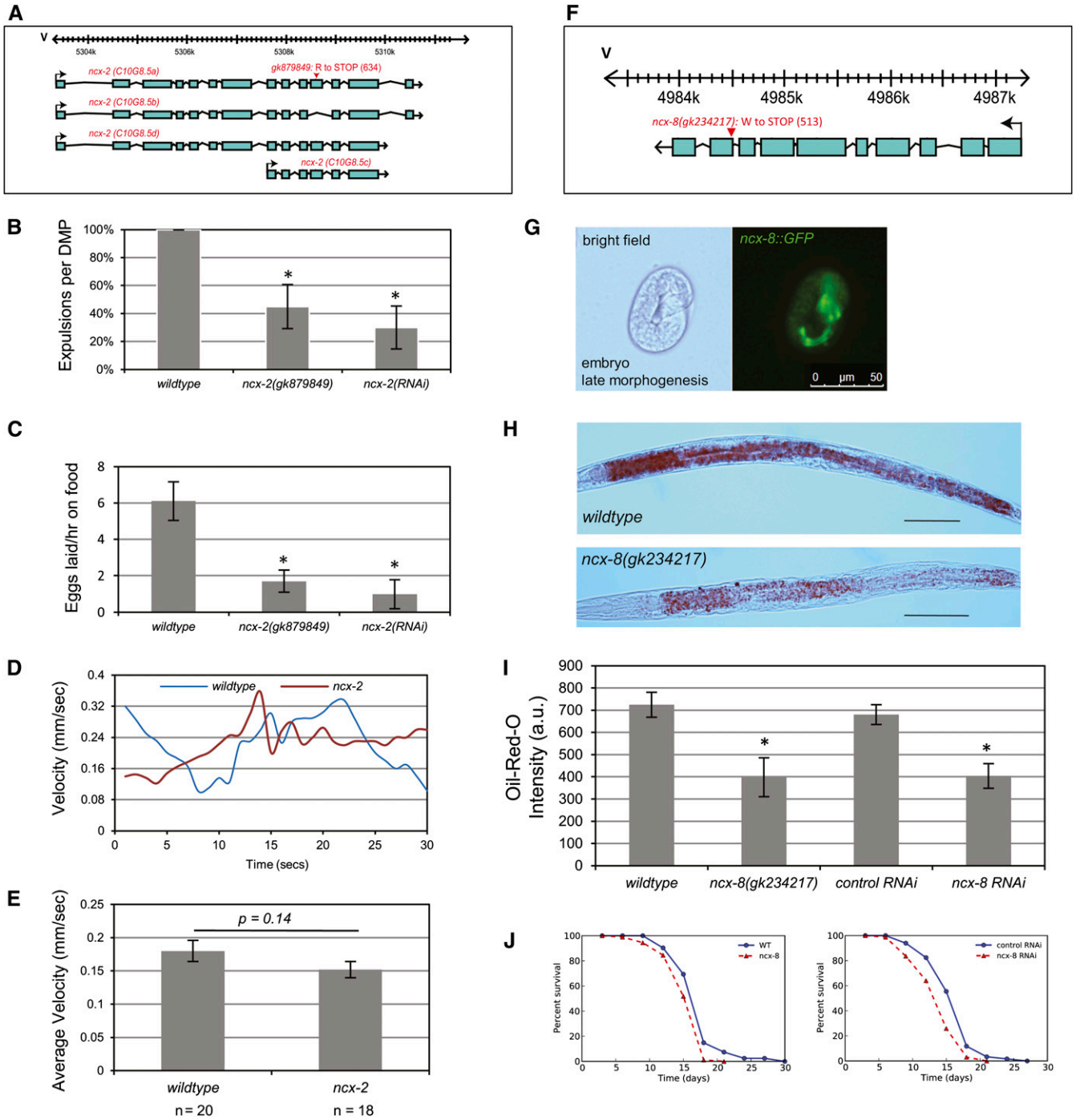

Figure 3 Characterization of the NCX transporter *ncx-2* and the CCX transporter *ncx-8*. (A) Predicted gene structure of the *ncx-2* splice forms on chromosome V. The amino acid position of the *gk879849* lesion is shown. The lesion in *gk879849* is defined by a premature opal stop codon at amino acid 634. (B) Bar chart of the percentage of expulsions per DMP cycle from 20 animals for wild-type animals, *ncx-2(gk879849)* mutant animals, and wild-type animals that were cultivated on bacteria expressing dsRNA targeting the *ncx-2* locus [*ncx-2(RNAi)*]. In the case of the *ncx-2* mutants, there is a significant defect in the number of expulsions per cycle when compared with wild-type animals at $P < 0.005$ for *ncx-2(gk879849)* mutant animals and *ncx-2(RNAi)* animals. (C) Bar chart of the average rate of egg laying per hour for wild-type, *ncx-2(gk879849)*, and wild-type animals that were cultivated on bacteria expressing dsRNA targeting the *ncx-2* locus [*ncx-2(RNAi)*]. Error bars represent the S.E.M; $*P < 0.05$. For each genotype a sample size of 10 animals was obtained and the mean was calculated. (D) Representative plots of the velocity (mm/sec) for wild-type and *ncx-2(gk879849)* mutant animals when off food. The animals were transferred to an unseeded plate and allowed to roam for 10 min and then movies of movement were taken. (E) Bar chart of the average velocity for wild-type and *ncx-2(gk879849)* mutant animals when off food. Error bars represent the S.E.M. *P*-values were calculated using the Student's *t*-test. (F) Predicted gene structure of the *ncx-8* gene on chromosome V. The amino acid position of the lesion is highlighted for *ncx-8 (gk234217)*, and the lesion in *gk324217* is defined by a premature stop codon at amino acid 513. (G) Expression of the *ncx-8* gene during the embryonic late morphogenesis stage. Bright-field image of an embryo (left) and GFP image of the same embryo (right). (H) Oil-Red-O staining in the

(Figure 3, D and E). We recorded movies of wild-type and *ncx-2* mutant animals moving while off food to compute their velocity. Representative plots of velocity of an individual wild-type and *ncx-2(gk879849)* mutant animal are plotted in Figure 3D, and bars of the average velocity for wild type and *ncx-2(gk879849)* are graphed in Figure 3E. We did not observe a significant difference in movement speed between wild-type and *ncx-2* mutant animals. Next we attempted to characterize the *ncx-8(gk234217)* mutant (Figure 3F). We observed expression of *ncx-8* in the pharynx and intestine during late embryonic morphogenesis (Figure 3G) and reasoned that NCX-8 may be contributing to metabolic function in *C. elegans*. To test this, we examined lipid accumulation in animals using Oil-Red-O stain. Oil-Red-O is used to stain lipids in *C. elegans* (Figure 3H), and quantification of Oil-Red-O staining is used to measure lipid accumulation (O'Rourke *et al.* 2009). Wild-type animals and *ncx-8 (gk234217)* mutant animals were fixed and soaked in Oil-Red-O, followed by quantification of Oil-Red-O staining. In the case of the *ncx-8(gk234217)* mutant animals, we observed significantly lower Oil-Red-O staining (Figure 3I: $P < 0.05$). We also cultivated wild-type animals on plates with bacteria expressing dsRNA targeting the *ncx-8* gene and also cultivated wild-type animals on control plates with bacteria transformed with empty control vectors. In the case of the animals cultivated on the RNA interference (RNAi) plates targeting *ncx-8*, we observed significant decreases in Oil-Red-O staining as compared with the animals cultivated on the control plates (Figure 3I: $P < 0.05$). Mutations in metabolic processes have been shown to affect longevity in *C. elegans* (Crawford *et al.* 2007; Wang *et al.* 2008), and so we investigated the life span of *ncx-8(gk234217)* mutant animals at 20°. Here we observed a significant difference in the percentage of survival of *ncx-8(gk234217)* mutant animals as compared with wild-type animals (Figure 3J: $P < 0.005$ for *ncx-8* mutants *vs.* wild-type animals at 20°). We also cultivated wild-type animals on plates with bacteria expressing dsRNA targeting the *ncx-8* gene and, as a control, cultivated wild-type animals on control plates with bacteria transformed with empty control vectors. In the case of the animals cultivated on the RNAi plates against *ncx-8*, we observed a significant decrease in the percentage of survival compared with the animals cultivated on the control plates (Figure 3J: $P < 0.005$).

Discussion

Here we analyze the family of Na^+/Ca^{2+} exchangers in *C. elegans*. Our analysis places these transporters into a phylogenetic framework, provides a comprehensive guide to their expression patterns, and reveals details about their functional roles through mutant analysis. From these data it is clear that nematode NCX, NCKX, and CCX exchangers are widely expressed and evolutionarily conserved. Current data from mammalian NCX exchangers show that these proteins function in muscles, neuronal cells, and renal tissue. Mammalian NCX1 exhibits expression in cardiac muscle, neuronal tissue, and the kidneys (Philipson *et al.* 2002; Nicoll *et al.* 2007; Valsecchi *et al.* 2013). NCX2 and NCX3 are expressed in skeletal muscle and neuronal cells (Li *et al.* 1994; Nicoll *et al.* 1996; Lytton 2007). The mammalian NCKX exchangers are more widely expressed in various cell types including photoreceptor cells, retinal ganglion cells, platelets, vascular smooth muscle, uterine tissue, intestinal cells, lung tissue, thymus, and epidermal cells (Lytton *et al.* 2002; Cai and Lytton 2004a; Lytton 2007; Visser and Lytton 2007; Altimimi *et al.* 2013). The CCX protein in humans is also very widely expressed in neurons, cardiac cells, skeletal muscle, lungs, kidneys, intestinal cells, and testes (Cai and Lytton 2004b). There are examples of tissue and cell-type specificity within the NCKX branch of mammals: for example, NCKX2 has been reported only in photoreceptors cells, retinal ganglion cells, and other neurons of the brain (Li *et al.* 1994). So within both NCX and NCKX there are broadly utilized exchangers and also regionally specified exchangers. Within the *C. elegans* Na^+/Ca^{2+} exchanger family we observe a similar pattern. Both NCX and CCX exchangers exhibit diverse expression patterns, but within each branch there are also more narrowly tuned exchangers. For example, the NCX gene *ncx-2* was detected only in muscle cells, while *ncx-1* and *ncx-3* were observed only in neuronal cell types. Similarly within the CCX branch, the *ncx-8* gene was observed in both muscle cells and intestinal cells. The other CCX genes, *ncx-6*, *ncx-7*, *ncx-9*, and *ncx-10*, were observed in both neuronal cells and other cell types (Table 1). Interestingly, in the case of the NCKX genes we observed tissue specificity as *ncx-4* and *ncx-5* were observed only in neuronal cells. Overall, the wide expression pattern observed for mammalian Na^+/Ca^{2+} exchangers is also true for *C. elegans* and shows a similar overall bias toward excitable cells.

intestine of a wild-type animal (top) and *ncx-8(gk324217)* mutant animal (bottom). The *ncx-8(gk324217)* mutant exhibits less Oil-Red-O staining. Oil-Red-O is used as a read-out for lipid accumulation in *C. elegans* (O'Rourke *et al.* 2009). Bar, 100 μm. (I) Quantification of Oil-Red-O staining in wild-type, *ncx-8(gk234217)* mutant animals, wild-type animals that were fed an empty control vector (L4440), and wild-type animals that were fed bacteria expressing dsRNA targeting the *ncx-8* locus. In the case of the *ncx-8(gk234217)* mutants and the animals that were fed RNAi clones targeting the *ncx-8* locus, the average Oil-Red-O staining is significantly lower when compared to wild-type animals or wild-type animals that were fed the control RNAi vector. *P*-values were calculated using the Student's *t*-test. Error bars represent the S.E.M.; $*P < 0.05$. (J) Longevity assays of *ncx-8(gk234217)* mutant animals and wild-type animals at 20°C (left), and longevity assays of wild-type animals cultivated on control RNAi plates and RNAi plates targeting the *ncx-8* locus (right). In each case a significant difference in survival was observed as compared with controls: $P < 0.005$ for *ncx-8* mutants *vs.* wild-type animals at 20°C, and $P < 0.005$ for wild-type animals cultivated on control RNAi plates compared with wild-type animals cultivated on *ncx-8* RNAi plates at 20°C. The *P*-values were calculated from log-rank tests.

Within *Drosophila* there are three characterized Na^+/Ca^{2+} exchangers, two of which belong to the NCKX branch and one of which belongs to the NCX branch. In the case of the NCKX gene *nckx-x* (*nckx-x-SC* in Figure 1A), neuronal expression has been observed throughout the nervous system and also in the eye-antennal disc, mushroom body, embryonic brain, and ventral nerve cord (Winkfein *et al.* 2004). The NCKX gene *nckx30c* is also widely expressed in neuronal cells of the brain and also in the craniofacial tissue, renal cells, and abdomen (Haug-Collet *et al.* 1999). The NCX gene in *Drosophila*, *Calx*, has been reported to be expressed only in photoreceptor cells (Schwarz and Benzer 1997; Webel *et al.* 2002). Through our phylogenetic analysis we also detected four uncharacterized CCX candidates in *Drosophila* (Figure 1A), and the precise expression of these genes is yet to be determined. By examining the family of Na^+/Ca^{2+} exchangers in three different systems, we now have data suggesting that Na^+/Ca^{2+} exchangers are represented by both a broadly tuned more general cohort and a more narrowly tuned and specified subset. However, exactly how these differences are regulated and how these differences in expression pattern map onto functional specializations is an unresolved question.

Acknowledgments

We thank Anthony LaMantia, John Hawdon, Sally Moody, Mary Ann Stepp, and Piali Sengupta for advice and insightful comments; Theresa Stiernagle and Aric Daul for the CGC strains used; the Moerman and Waterston labs and Million Mutation Project team for mutants; our anonymous reviewers for suggestions and feedback; and Thomas Maynard and Anastas Popratiloff for imaging advice. Funding was provided by The George Washington University Department of Biological Sciences and Columbian College of Arts and Sciences (to V.S., C.H., Z.M., and D.O.); The George Washington University Luther Rice Undergraduate Research Fellowship (to E.B.); and The George Washington University Department of Biological Sciences Wilbur V. Harlan Scholarship Trust (to J.S.).

Literature Cited

Altimimi, H. F., R. T. Szerencsei, and P. P. Schnetkamp, 2013 Functional and structural properties of the NCKX2 na (+)-ca (2+)/K (+) exchanger: a comparison with the NCX1 na (+)/ca (2+) exchanger. Adv. Exp. Med. Biol. 961: 81–94.

Berridge, M. J., P. Lipp, and M. D. Bootman, 2000 The versatility and universality of calcium signalling. Nat. Rev. Mol. Cell Biol. 1: 11–21.

Berridge, M. J., M. D. Bootman, and H. L. Roderick, 2003 Calcium signalling: dynamics, homeostasis and remodelling. Nat. Rev. Mol. Cell Biol. 4: 517–529.

Bootman, M. D., P. Lipp, and M. J. Berridge, 2001 The organisation and functions of local ca(2+) signals. J. Cell Sci. 114: 2213–2222.

Cai, X., and J. Lytton, 2004a The cation/ca(2+) exchanger superfamily: phylogenetic analysis and structural implications. Mol. Biol. Evol. 21: 1692–1703.

Cai, X., and J. Lytton, 2004b Molecular cloning of a sixth member of the K+-dependent na+/Ca2+ exchanger gene family, NCKX6. J. Biol. Chem. 279: 5867–5876.

Coates, J. C., and M. de Bono, 2002 Antagonistic pathways in neurons exposed to body fluid regulate social feeding in Caenorhabditis elegans. Nature 419: 925–929.

Crawford, D., N. Libina, and C. Kenyon, 2007 Caenorhabditis elegans integrates food and reproductive signals in lifespan determination. Aging Cell 6: 715–721.

Gray, J. M., D. S. Karow, H. Lu, A. J. Chang, J. S. Chang *et al.*, 2004 Oxygen sensation and social feeding mediated by a C. elegans guanylate cyclase homologue. Nature 430: 317–322.

Gray, J. M., J. J. Hill, and C. I. Bargmann, 2005 A circuit for navigation in Caenorhabditis elegans. Proc. Natl. Acad. Sci. USA 102: 3184–3191.

Haug-Collet, K., B. Pearson, R. Webel, R. T. Szerencsei, R. J. Winkfein *et al.*, 1999 Cloning and characterization of a potassium-dependent sodium/calcium exchanger in Drosophila. J. Cell Biol. 147: 659–670.

Hilge, M., 2012 Ca2+ regulation of ion transport in the na+/Ca2+ exchanger. J. Biol. Chem. 287: 31641–31649.

Li, Z., S. Matsuoka, L. V. Hryshko, D. A. Nicoll, M. M. Bersohn *et al.*, 1994 Cloning of the NCX2 isoform of the plasma membrane na(+)-Ca2+ exchanger. J. Biol. Chem. 269: 17434–17439.

Lytton, J., 2007 Na+/Ca2+ exchangers: Three mammalian gene families control Ca2+ transport. Biochem. J. 406: 365–382.

Lytton, J., X. F. Li, H. Dong, and A. Kraev, 2002 K+-dependent na+/Ca2+ exchangers in the brain. Ann. N. Y. Acad. Sci. 976: 382–393.

Nicoll, D. A., B. D. Quednau, Z. Qui, Y. R. Xia, A. J. Lusis *et al.*, 1996 Cloning of a third mammalian na+-Ca2+ exchanger, NCX3. J. Biol. Chem. 271: 24914–24921.

Nicoll, D. A., X. Ren, M. Ottolia, M. Phillips, A. R. Paredes *et al.*, 2007 What we know about the structure of NCX1 and how it relates to its function. Ann. N. Y. Acad. Sci. 1099: 1–6.

Nicoll, D. A., M. Ottolia, J. I. Goldhaber, and K. D. Philipson, 2013 20 years from NCX purification and cloning. Milestones. Adv. Exp. Med. Biol. 961: 17–23.

O'Rourke, E. J., A. A. Soukas, C. E. Carr, and G. Ruvkun, 2009 C. elegans major fats are stored in vesicles distinct from lysosome-related organelles. Cell Metab. 10: 430–435.

Ottolia, M., and K. D. Philipson, 2013 NCX1: Mechanism of transport. Adv. Exp. Med. Biol. 961: 49–54.

Philipson, K. D., and D. A. Nicoll, 2000 Sodium-calcium exchange: A molecular perspective. Annu. Rev. Physiol. 62: 111–133.

Philipson, K. D., D. A. Nicoll, M. Ottolia, B. D. Quednau, H. Reuter *et al.*, 2002 The na+/Ca2+ exchange molecule: An overview. Ann. N. Y. Acad. Sci. 976: 1–10.

Sambongi, Y., T. Nagae, Y. Liu, T. Yoshimizu, K. Takeda *et al.*, 1999 Sensing of cadmium and copper ions by externally exposed ADL, ASE, and ASH neurons elicits avoidance response in caenorhabditis elegans. Neuroreport 10: 753–757.

Schwarz, E. M., and S. Benzer, 1997 Calx, a na-ca exchanger gene of drosophila melanogaster. Proc. Natl. Acad. Sci. USA 94: 10249–10254.

Thomas, J. H., 1990 Genetic analysis of defecation in *Caenorhabditis elegans*. Genetics 124: 855–872.

Tidow, H., L. R. Poulsen, A. Andreeva, M. Knudsen, K. L. Hein *et al.*, 2012 A bimodular mechanism of calcium control in eukaryotes. Nature 491: 468–472.

Troemel, E. R., J. H. Chou, N. D. Dwyer, H. A. Colbert, and C. I. Bargmann, 1995 Divergent seven transmembrane receptors are candidate chemosensory receptors in C. elegans. Cell 83: 207–218.

Valsecchi, V., G. Pignataro, R. Sirabella, C. Matrone, F. Boscia *et al.*, 2013 Transcriptional regulation of ncx1 gene in the brain. Adv. Exp. Med. Biol. 961: 137–145.

Visser, F., and J. Lytton, 2007 K+ -dependent na+/Ca2+ exchangers: Key contributors to Ca2+ signaling. Physiology (Bethesda) 22: 185–192.

Wang, M. C., E. J. O'Rourke, and G. Ruvkun, 2008 Fat metabolism links germline stem cells and longevity in C. elegans. Science 322: 957–960.

Webel, R., K. Haug-Collet, B. Pearson, R. T. Szerencsei, R. J. Winkfein *et al.*, 2002 Potassium-dependent sodium-calcium exchange through the eye of the fly. Ann. N. Y. Acad. Sci. 976: 300–314.

Winkfein, R. J., B. Pearson, R. Ward, R. T. Szerencsei, N. J. Colley *et al.*, 2004 Molecular characterization, functional expression and tissue distribution of a second NCKX na+/Ca2+ -K+ exchanger from drosophila. Cell Calcium 36: 147–155.

Communicating editor: P. Sengupta

GENETICS

Supporting Information
http://www.genetics.org/lookup/suppl/doi:10.1534/genetics.113.153106/-/DC1

Insight into the Family of Na^+/Ca^{2+} Exchangers of *Caenorhabditis elegans*

Vishal Sharma, Chao He, Julian Sacca-Schaeffer, Eric Brzozowski, Daniel E. Martin-Herranz, Zelda Mendelowitz, David A. Fitzpatrick, and Damien M. O'Halloran

DOI: 10.1534/genetics.113.153106

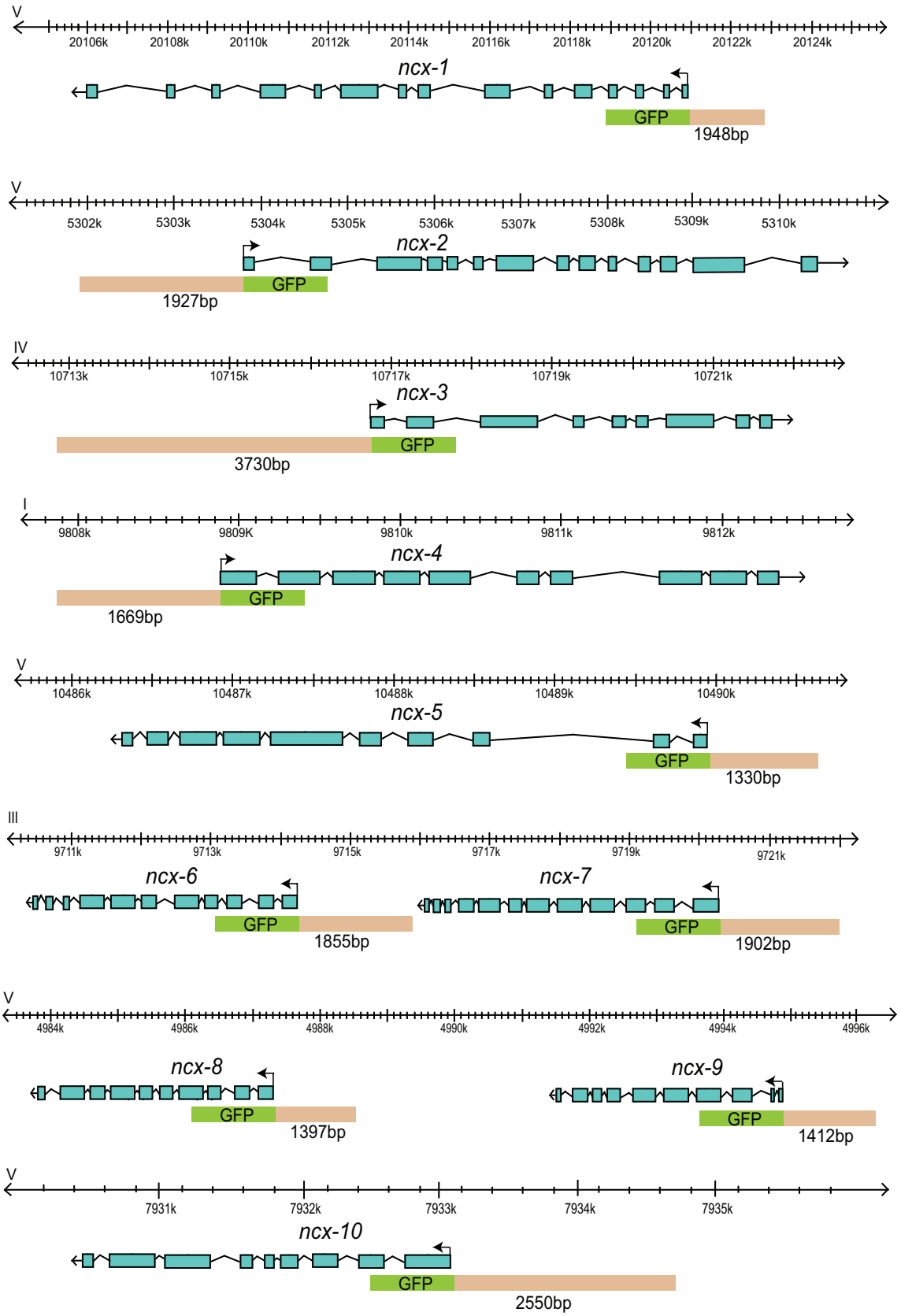

Figure S1 Promoter elements used in the GFP reporter fusions. Genomic loci were downloaded from Wormbase (www.wormbase.org). The promoter sequence for each gene that was PCR amplified is represented in beige and the GFP coding sequence is indicated in green.

File S1

Supplemental Materials and Methods

Animals and Maintenance

The following animals were used in our study: Bristol N2 (wildtype), DMH22 *ncx-2 (gk879849)*, DMH25 *ncx-8(gk234217)*, OH4350 *otIs151[(p)ceh-36::RFP; rol-6(su1006)]; otEx2504[(p)gcy-28::GFP; (p)unc-122::GFP],* DMH23 *otIs151[(p)ceh-36::RFP; rol-6(su1006)]; hanEx4[(p)ncx-4::GFP; (p)elt-2::GFP],* DA1290 *lin-15B(n765) X; adEx1290[(p)gcy-33::GFP + lin-15(+)],* OH7511 *otIs197[(p)unc14::hif-1(P621A); (p)ttx-3::RFP],* PY2417 *oyIs44[(p)odr-1::RFP],* ZG611 *isIs19[(p)gcy-32::GFP; unc-119(+)]*, DMH1 *hanEx4[(p)ncx-4::GFP; (p)elt-2::GFP],* DMH10 *hanEx2[(p)ncx-2::GFP]*, DMH9 *hanEx3[(p)ncx-3::GFP],* DMH12 *hanEx1[(p)ncx-1::GFP; (p)elt-2::GFP],* DMH6 *hanEx5[(p)ncx-5::GFP],* DMH13 *hanEx6[(p)ncx-6::GFP],* DMH14 *hanEx7[(p)ncx-7::GFP],* DMH11 *hanEx8[(p)ncx-8::GFP],* DMH15 *hanEx9[(p)ncx-9::GFP; (p)elt-2::GFP]*, DMH7 *hanEx10[(p)ncx-10::GFP; (p)elt-2::GFP]* - for more transgene details of the *ncx* reporters, refer to Table S1. In each case, multiple (between three and six) independent transgenic lines were examined for each reporter. The strain DMH22 was obtained by outcrossing the strain VC40914 two times through wildtype N2 animals, and similarly the strain DMH25 was obtained by outcrossing the strain VC40058 two times through N2 animals, and in each case homozygous mutants were selected by PCR and sequencing of the lesion. NGM plates were seeded with *E. coli* strain OP50 and maintained according to standard protocol (Brenner. 1974).

Phylogenetic Analysis

Genomes were downloaded from Wormbase (*Caenorhabditis* species - *C. briggsae*, *C. brenneri*, *C. japonica*, *C. remanei* - and *Pristionchus pacificus*), NCBI (*Drosophila*), and Ensembl (human), and interrogated for NCX, NCKX and CCX transporter sequences with bidirectional BlastP searches [>*blastall -p blastp –d.../...-e 0.00001*] using local Blast executables (ftp://ftp.ncbi.nlm.nih.gov/blast/executables/blast+/LATEST/) and motif scanning analysis. Orthologs were aligned using the multiple sequence alignment software MUSCLE v3.8.31 (Edgar. 2004), and gaps were systematically stripped after alignment. Phylogenetic relationships were inferred by reconstructing trees by Maximum Likelihood using the PhyML command-line application (Guindon and Gascuel. 2003). The appropriate model was selected using Prottest v3 (Abascal *et al*. 2005; Darriba *et al*. 2011) , and determined to be the "WAG+I+G+F" model with a fixed gamma distribution parameter of 1.5, the proportion of invariable sites set to 0.003, and four substitution rate categories. For completeness we also reconstructed Bayesian trees (data not shown) using MrBayes version 3.2 and obtained the same topology using the WAG model (Ronquist and Huelsenbeck. 2003). The analysis used a Markov Chain Monte Carlo (MCMC) method that ran for 2 million generations, sampled every 10th

generation. The *burnin* was set after examining the log probability of the data using the *sump* command, and clade probabilities for each phylogeny were determined using the *sumt* command. Protein structure of Na^+/Ca^{2+} exchangers in *C. elegans* was predicted using SMART (http://smart.embl-heidelberg.de/) and InterPro (http://www.ebi.ac.uk/interpro) databases, and the TM-Finder program (http://tmfinder.research.sickkids.ca/cgi-bin/TMFinderForm).

Generation of GFP Reporter Gene Fusions

The transcriptional GFP reporter fusions were made by PCR fusion as described previously (Boulin *et al*. 2006) . The promoter sequence (see Figure S1) was amplified by PCR using High Fidelity polymerase (Roche). A GFP coding region which contained the *unc-54* 3'UTR was PCR amplified from the plasmid pPD95.75 (available from AddGene: http://www.addgene.org/1494/) using the primers:

GFP-F: AGCTTGCATGCCTGCAGGTCGACT

GFP-R: AAGGGCCCGTACGGCCGACTAGTAGG

Following PCR amplification and purification of the promoter and GFP fragment, a fusion PCR step was performed using 10ng of each amplicon with a nested promoter specific primer (see Table S1) and the nested primer:

GFP nested primer: GGAAACAGTTATGTTTGGTATATTGGG

The resulting PCR fusions were PCR purified and micro-injected at between 30-100ng/µl into the germ-line of wildtype (N2) animals.

Reporter Gene Expression Analysis and Cell Identification

The transcriptional GFP reporter fusions were injected into wildtype (N2) animals and stable lines selected and maintained. Stable transgenic lines were imaged using a Zeiss LSM 710 system confocal microscope under 20X and 63X magnification. Neuronal cell identification was confirmed using reporter lines, using dye-filling assays, and also inferred from position and morphology (including cilia structure, and cell body shape). The lipophilic dye DiD (Invitrogen) has been used to visualize specific neurons (ASI, ADL, ASK, AWB, ASH, and ASJ amphid neurons, and also the PHA and PHB phasmid neurons) (Inglis *et al*. 2007) . DiD was eluted in 2.5ml of dimethylformamide (DMF) to obtain a stock solution of 10mg/ml. Worms were washed from *E. coli* strain OP50 seeded plates two times in M9 solution and exposed to DiD dye (1:1000 dilution of stock) on a rotator for 2 hrs. The worms were then washed two times in M9 and allowed to recover on an OP50 seeded plate for 1 hour. The animals were then washed off the plate two times in ddH_20 and examined using TRITC filters. In the case of the *(p)ncx-1*::GFP expressing animals, cells were identified by crossing into the transgenic line OH7511 which expresses soluble RFP in the AIY interneuron

((*p)ttx-3*::RFP). The *(p)ncx-4*::GFP expressing animals were crossed into the transgenic line OH4350, which was previously selected against the extra-chromosomal array *otEx2504*, and thereby retained only animals containing the *otIs51* transgene which expresses soluble RFP in the AWC and ASE neurons; this line was named DMH23. For *(p)ncx-5*::GFP expressing animals, the transgenic lines ZG611and DA1290 were used to compare expression patterns; ZG611 animals harbor a transgene expressing soluble GFP under the *gcy-32* promoter in the URX, PQR, and AQR cells, and DA1290 animals express soluble GFP under the *gcy-33* promoter (BAG cell reporter). The ADL neuron was identified as a site of expression for *(p)ncx-6*::GFP and *(p)ncx-7*::GFP fusions based upon the distinctive 'tuning-fork' shaped cilia, and also by testing positive for DiD dye overlap.

Defecation Motor Program Assays

To examine the DMP cycle we measured the number of expulsions per DMP cycle time by examining day1 adult animals under a dissecting microscope. The DMP cycle in *C. elegans* represents a stereotyped intrinsic rhythm that occurs every ~45secs (Thomas. 1990; Xing *et al*. 2008) . For each genotype 20 animals were screened. For RNAi experiments, animals were grown from eggs to day 1 of adulthood on *E. coli* expressing dsRNA specific to the *ncx-2* gene (CUUkp3304M134Qclone, SourceBioscience). The RNAi insert clone was sequence verified prior to use. NGM plates for RNAi experiments contained standard NGM recipe and also 25µg/ml Carbenicillin and 1mM IPTG.

Egg-laying Assays

To quantify the rate of egg-laying, L4 stage animals were picked onto staging plates seeded with *E. coli* strain OP50 and 24hrs later an individual day 1 adult animal was transferred to a seeded plate for two hours at room temperature. The number of eggs laid during this time was counted by examining the plate under a dissection microscope. This was repeated ten times for each genotype. For RNAi experiments, animals were grown from eggs to day 1 of adulthood on *E. coli* expressing dsRNA specific to the *ncx-2* gene (CUUkp3304M134Q clone, SourceBioscience) and then transferred individually to a seeded NGM plate for 2hrs. The average number of fertilized eggs within each animal for *ncx-2(gk879849)* mutant animals and wildtype animals was compared by counting the number of unlaid eggs in ten individual day 1 adults.

Tracking Worm Movement

Movies of worms were captured using a Leica IC80 HD digital microscope camera connected to a Leica M165F dissecting microscope and visualized through a HDMI connection into an adjacent monitor. Movies were captured as mp4 files and converted to TIFF series using the ffMPEG Binary (only available on a MAC) at this URL -http://ffmpegmac.net/.

Files were converted and extracted using the following command line:

> ffmpeg -y -i sample.mp4 -an -r 3 -pix_fmt rgb24 -vcodec tiff tif/%010d.tif

Prior to capturing movies, animals were grown to the L4 stage at room temperature and transferred to a separate *E. coli* strain OP50 seeded plate at room temperature. 24hrs later day 1 adult animals were picked from this plate onto an unseeded NGM plate and allow to roam for 10mins. After this time movies were recorded of their movement over ~60secs. Analysis of movement was performed using the '*manual tracking*' (http://rsbweb.nih.gov/ij/plugins /track/track.html) and '*wrmtrk*' (http://www.phage.dk/plugins/wrmtrck.html) plugins in *ImageJ* (http://rsb.info.nih.gov/ij/).

Quantification of Oil-Red-O Staining

Oil-Red-O staining of lipid accumulation was performed as described previously (O'Rourke *et al*. 2009) . Oil-Red-O (O0625 Sigma) was prepared by adding 0.5g of Oil-Red-O into 100ml of isopropanol. This solution was equilibrated for three days by stirring at room temperature and then diluted to 60% in ddH_20 and filtered using a 0.2μm filter. 10 L4 staged animals were transferred to a seeded (*E. coli* strain OP50) NGM staging plate at room temperature and 24hours later the day 1 adult animals were transferred to multiple seeded (*E. coli* strain OP50) NGM plates and allowed to lay eggs for 8hrs and then each individual adult animal was removed. The plates were left at room temperature until the progeny grew to the L4 stage. The *ncx-8* gene is expressed in the intestine from embryogenesis (Figures 2H and 3G), and so L4 stage animals were fixed and quantified so as to permit intestinal quantification and avoid staining of the germ-line. Animals were collected and washed in 1X PBS prior to fixation and reduction and then soaked in Oil-Red-O dye overnight on a rotator and then washed in 1X PBS and placed onto microscope slides for imaging using a Zeiss LSM 710 system confocal microscope. Whole body Oil-Red-O staining was then quantified using *ImageJ* software to obtain the mean staining intensity for between 15 and 20 animals in each experiment. For RNAi experiments, animals were cultivated from eggs to L4 stage on *E. coli* expressing either an empty control vector (L4440, Addgene) or the L4440 vector expressing dsRNA specific to the *ncx-8* gene (CUUkp3304C014Q clone, SourceBioscience). The RNAi insert clone was sequence verified prior to use. NGM plates for RNAi experiments contained standard NGM recipe and also 25μg/ml Carbenicillin and 1mM IPTG.

Longevity Assays

Animals were synchronized by a timed egg laying (TEL), and cultivated on NGM plates seeded with *E. coli* strain OP50 at 20ºC. The L4 stage was set as Day 0 and the next Day (i.e. adult Day 1) was set as Day 1. Longevity assays were conducted and measured as described previously (Apfeld and Kenyon. 1999). Animals were transferred every few days to fresh NGM seeded

plates at 20ºC and the number of dead animals scored. FuDR was not used in the NGM plates to avoid confounding our results (Aitlhadj and Sturzenbaum. 2010). Survival curves and statistics were analyzed using OASIS (Yang *et al*. 2011) . The Log-Rank test was used to infer significance. Number of dead worms, not including censored animals, was: 79(N2), 87(*ncx-8*), 69(control RNAi), 109(*ncx-8* RNAi). For RNAi experiments, animals were grown on *E. coli* expressing either an empty control vector (L4440, Addgene) or the L4440 vector expressing dsRNA targeting the *ncx-8* gene (CUUkp3304C014Q clone, SourceBioscience).

SUPPLEMENTAL LITERATURE CITED

Abascal, F., R. Zardoya and D. Posada, 2005 ProtTest: Selection of best-fit models of protein evolution. Bioinformatics **21:** 2104-2105.

Aitlhadj, L., and S. R. Sturzenbaum, 2010 The use of FUdR can cause prolonged longevity in mutant nematodes. Mech. Ageing Dev. **131:** 364-365.

Apfeld, J., and C. Kenyon, 1999 Regulation of lifespan by sensory perception in caenorhabditis elegans. Nature **402:** 804-809.

Boulin, T., J. F. Etchberger and O. Hobert, 2006 Reporter gene fusions. WormBook 1-23.

Brenner, S., 1974 The genetics of caenorhabditis elegans. Genetics **77:** 71-94.

Darriba, D., G. L. Taboada, R. Doallo and D. Posada, 2011 ProtTest 3: Fast selection of best-fit models of protein evolution. Bioinformatics **27:** 1164-1165.

Edgar, R. C., 2004 MUSCLE: Multiple sequence alignment with high accuracy and high throughput. Nucleic Acids Res. **32:** 1792-1797.

Guindon, S., and O. Gascuel, 2003 A simple, fast, and accurate algorithm to estimate large phylogenies by maximum likelihood. Syst. Biol. **52:** 696-704.

Inglis, P. N., G. Ou, M. R. Leroux and J. M. Scholey, 2007 The sensory cilia of caenorhabditis elegans. WormBook 1-22.

O'Rourke, E. J., A. A. Soukas, C. E. Carr and G. Ruvkun, 2009 C. elegans major fats are stored in vesicles distinct from lysosome-related organelles. Cell. Metab. **10:** 430-435.

Ronquist, F., and J. P. Huelsenbeck, 2003 MrBayes 3: Bayesian phylogenetic inference under mixed models. Bioinformatics **19:** 1572-1574.

Thomas, J. H., 1990 Genetic analysis of defecation in caenorhabditis elegans. Genetics **124:** 855-872.

Xing, J., X. Yan, A. Estevez and K. Strange, 2008 Highly Ca2+-selective TRPM channels regulate IP3-dependent oscillatory Ca2+ signaling in the C. elegans intestine. J. Gen. Physiol. **131:** 245-255.

Yang, J. S., H. J. Nam, M. Seo, S. K. Han, Y. Choi *et al*, 2011 OASIS: Online application for the survival analysis of lifespan assays performed in aging research. PLoS One **6:** e23525.

Table S1 PCR Primers used to generate reporter GFP constructs

Primers				Resulting Transgenic Arrays
Promoter	F1	F-Nested	Reverse	
ncx-1	ACTTTCACCTTTTCTTCTCCATCTCCTC	GAAACTCTGACTTCCAGGTTGATTTTGG	AGTCGACCTGCAGGCATGCAAGCTCGCATTTGTAGTTGTCTCTGGAAAAAAATT	*hanEx1*
ncx-2	TCCTTCATTTTAAAACTCCACGGCCAAG	TCCTTCATTTTAAAACTCCACGGCCAAG	AGTCGACCTGCAGGCATGCAAGCTTCAACTGAAAATCAGATTTTAGGCTTTTAA	*hanEx2*
ncx-3	CTTCACACAAAAGCTCAACGGTACTTTC	CTGCATCTCCTGCTCTCTCCTTACATTA	AGTCGACCTGCAGGCATGCAAGCTGTTTGATCCTGAAAGTAATAAAAACTTTTA	*hanEx3*
ncx-4	TGGTGGTACGTCATAATCCAGTCTCAAG	TGTAGTAGATCCTCCTCCCCGCCTTTTT	AGTCGACCTGCAGGCATGCAAGCTTATTTTTAAAAATCAAAATATGATAATTTG	*hanEx4*
ncx-5	ATGTTTGAAATTGGGGAATGAATGCAAAA	AGTCGATGCGGAGAAATGTCTGAAGCCAAA	AGTCGACCTGCAGGCATGCAAGCTCTTTTGAAATACTCAACTCACATTCCGGAT	*hanEx5*
ncx-6	CAACCGTAATATCCCCTGAGATCAATAA	CATAGATGCGAACAATTTTCAACAAAAA	AGTCGACCTGCAGGCATGCAAGCTTGATACAAAAATTGACCTGAAAACTTTAAAA	*hanEx6*
ncx-7	AAAAGATGTTCCTTCGATGCCTGACCTC	CTGCTGCTGCTGATTATGCTCTTTTGGT	AGTCGACCTGCAGGCATGCAAGCTAACATAGATCTGAAAATGTTTAAAATAAGA	*hanEx7*
ncx-8	ACTCATTTTTTGCCGTGCCTATCGTTCAT	GATCAAAGACACGAGGTAGCGAATTCCA	AGTCGACCTGCAGGCATGCAAGCTGAGAAGGAGTTTGAAATTTAGTTGAAACGA	*hanEx8*
ncx-9	AACACAGCGCAAGTAGCAAGTAGCAAGT	CTCAATTCCTTTCCACCACTCACTGAAC	AGTCGACCTGCAGGCATGCAAGCTTTCCTCATCAAAAGGGAATCCATCATAAAT	*hanEx9*
ncx-10	GTTCTTTCAACATTGCAAAAAGGCACCA	TACACAGTTGCAGAGGCGTTTAATCAGA	AGTCGACCTGCAGGCATGCAAGCTACCTGAAAAAGAAACAGTTGATAAGCGGGT	*hanEx10*